TOXICOLOGICAL SCIENCES, 146(1), 2015, 89–100

doi: 10.1093/toxsci/kfv072
Advance Access Publication Date: April 13, 2015
Research Article

NOS-2 Inhibition in Phosgene-Induced Acute Lung Injury

Piotr T. Filipczak[*,†], Albert P. Senft[*], JeanClare Seagrave[*], Waylon Weber[*], Philip J. Kuehl[*], Laura E. Fredenburgh[†], Jacob D. McDonald[*], and Rebecca M. Baron[†,1]

[*]Environmental Respiratory Health and Chemistry and Inhalation Exposure Programs, Lovelace Respiratory Research Institute, Albuquerque, New Mexico 87108 and [†]Department of Medicine, Division of Pulmonary and Critical Care Medicine, Brigham & Women's Hospital, Harvard Medical School, Boston, Massachusetts 02115

[1]To whom correspondence should be addressed at Department of Medicine, Division of Pulmonary and Critical Care Medicine, Brigham & Women's Hospital, Harvard Medical School, Boston, Massachusetts 02115. E-mail: rbaron@partners.org.

ABSTRACT

Phosgene exposure *via* an industrial or warfare release produces severe acute lung injury (ALI) with high mortality, characterized by massive pulmonary edema, disruption of epithelial tight junctions, surfactant dysfunction, and oxidative stress. There are no targeted treatments for phosgene-induced ALI. Previous studies demonstrated that nitric oxide synthase 2 (NOS-2) is upregulated in the lungs after phosgene exposure; however, the role of NOS-2 in the pathogenesis of phosgene-induced ALI remains unknown. We previously demonstrated that NOS-2 expression in lung epithelium exacerbates inhaled endotoxin-induced ALI in mice, mediated partially through downregulation of surfactant protein B (SP-B) expression. Therefore, we hypothesized that a selective NOS-2 inhibitor delivered to the lung epithelium by inhalation would mitigate phosgene-induced ALI. Inhaled phosgene produced increases in bronchoalveolar lavage fluid protein, histologic lung injury, and lung NOS-2 expression at 24 h. Administration of the selective NOS-2 inhibitor 1400 W *via* inhalation, but not *via* systemic delivery, significantly attenuated phosgene-induced ALI and preserved epithelial barrier integrity. Furthermore, aerosolized 1400 W augmented expression of SP-B and prevented downregulation of tight junction protein zonula occludens 1 (ZO-1), both critical for maintenance of normal lung physiology and barrier integrity. We also demonstrate for the first time that NOS-2-derived nitric oxide downregulates the ZO-1 expression at the transcriptional level in human lung epithelial cells, providing a novel target for ameliorating vascular leak in ALI. Our data demonstrate that lung NOS-2 plays a critical role in the development of phosgene-induced ALI and suggest that aerosolized NOS-2 inhibitors offer a novel therapeutic strategy for its treatment.

Key words: phosgene; acute lung injury; nitric oxide synthase 2; lung epithelium; surfactant protein B; tight junction protein 1

INTRODUCTION

Acute respiratory distress syndrome (ARDS) is a life-threatening disorder affecting approximately 200 000 people per year in the United States (Matthay and Zemans, 2011). ARDS is characterized by acute bilateral pulmonary infiltrates not attributable to heart failure and severe hypoxemia resulting in respiratory failure. Increases in oxidative stress, upregulation of cytokines and chemokines, recruitment of inflammatory cells, and upregulation of proinflammatory signaling molecules lead to epithelial and endothelial cell injury, surfactant dysfunction, and loss of alveolar epithelial barrier integrity (Cortes *et al.*, 2012; Matthay and Zemans, 2011). A variety of factors and clinical conditions underlie ARDS, most commonly sepsis, pneumonia, mechanical ventilation, aspiration of gastric contents, and inhalation of toxic substances. Despite decades of research, ARDS treatment remains limited to supportive care, including treatment of the underlying etiology, protective ventilation strategies (low tidal volume ventilation), neuromuscular blockade, and prone positioning (Fan et al., 2013; Guerin et al., 2013; Papazian et al., 2010; Shafeeq and Lat, 2012). Mortality rates remain unacceptably high at 34–55% (Saguil and Fargo, 2012).

Phosgene ($COCl_2$), a highly toxic and reactive gas classified as a chemical warfare agent, induces severe ARDS with high mortality. Phosgene is a component in the synthesis of organic chemicals including isocyanates and polycarbonates, and approximately 5 million metric tons are produced annually worldwide (Pauluhn et al., 2007). Thus, phosgene poses a significant threat of mass casualties in the event of a terrorist attack or industrial accident. Phosgene toxicity is mediated through acetylation of hydroxyl, thiol, amine, and sulfhydryl groups of proteins, carbohydrates, and lipids within the lung (Grainge and Rice, 2010; Pauluhn et al., 2007). ARDS induced by phosgene is characterized by increased oxidative stress resulting in massive pulmonary edema, fibrinocellular alveolitis, and hypoxemia. These deleterious changes are produced through alveolar and vascular leak, disruption of epithelial tight junctions, surfactant dysfunction, and inflammation triggered by release of arachidonic acid mediators such as leukotrienes (Brown et al., 2002; Guo et al., 1990; Pauluhn et al., 2007). Treatment for phosgene-induced lung injury has focused on mitigating oxidative injury and inflammation using corticosteroids and β-agonists, as well as mechanical ventilation (Grainge and Rice, 2010). These approaches have demonstrated limited therapeutic efficacy; therefore, development of new treatments that target novel pathways remains necessary.

An important mediator of acute lung injury (ALI) is nitric oxide (NO) synthase 2 (NOS-2), an enzyme upregulated in ARDS patients as well as in animal ALI models (Baron et al., 2004a, b; Mehta, 2005). Recent studies demonstrate that NOS-2 is induced in rat lungs exposed to phosgene (Chen et al., 2013; Zhang et al., 2012). Additionally, recent work has shown that the potential efficacy of ethyl pyruvate and melatonin in rats exposed to phosgene is secondary to downregulation of NOS-2 expression (Chen et al., 2013; Zhang et al., 2012), suggesting that NOS-2 may contribute to phosgene-induced ALI. Still, little is known regarding the role of NOS-2 in phosgene-induced ALI nor its value as a therapeutic target. Although endogenous NOS-2 expression in the lung is low, it is highly inducible with inflammatory or toxic stimuli, such as cytokines (interferon-γ, TNF-α, IL-1β), bacteria and their products (lipopolysaccharide), or toxic chemicals (chlorine) (Martin et al., 2003; Zhang et al., 2013). Selective inhibition or deficiency of NOS-2 has been shown to attenuate inflammation, oxidative stress, surfactant dysfunction, vascular leak, and physiologic lung dysfunction in several animal models of nonchemically induced ALI (Baron et al., 2004a, b; Mehta, 2005). However, conflicting results suggested differential effects on NOS-2 expression with respect to individual cell types depending on the model of lung injury (Baron et al., 2004a; Pheng et al., 1995).

We previously showed that NOS-2 induction in lung epithelium plays an important role in the development of ALI and physiologic lung dysfunction in endotoxin-induced ALI in mice (Baron et al., 2004a). Although NO can cause surfactant dysfunction through direct interactions with surfactant lipid or protein components (Haddad et al., 1993), we demonstrated that NOS-2-derived NO transcriptionally downregulates SP-B expression and promoter activity in lung epithelial cells (Baron et al., 2004a). The aim of this study was to determine whether selective inhibition of NOS-2 in lung epithelium ameliorates phosgene-induced ALI, and therefore, whether NOS-2 inhibition may be therapeutic for phosgene-induced ALI. We used the selective NOS-2 inhibitor 1400 W, demonstrated to be 5000- and 200-fold more potent against human purified NOS-2 than against eNOS and nNOS, respectively (Garvey et al., 1997). Our results demonstrate that aerosolized 1400 W significantly attenuates phosgene-induced ALI and suggest that inhalational delivery of a NOS-2-specific inhibitor offers a novel therapy to treat phosgene-induced ARDS.

MATERIALS AND METHODS

In vivo studies. The studies were performed under the Lovelace Respiratory Research Institute (LRRI)-approved Institutional Animal Care and Use Committee (IACUC) protocol. Female 6-week old C57BL/6 mice were purchased from Jackson Laboratory and used for experiments after 2 weeks of quarantine at the age of 8 weeks. Previous literature reported no gender-specific susceptibilities to phosgene (Pauluhn 2006). The animals were housed in a temperature-controlled environment (24–26°C) with constant humidity (55–60%) and controlled photoperiod (12-h light/dark cycle). The mice were randomly divided into 5 experimental groups: (i) filtered air, (ii) phosgene + subcutaneous (SQ) vehicle, (iii) phosgene + SQ 1400 W, (iv) phosgene + aerosolized vehicle and (v) phosgene + aerosolized 1400 W. The numbers of animals per group are provided in the figure legends. Phosphate-buffered saline (PBS) was used as the vehicle. Mice were exposed to phosgene (5 ppm *via* nose only inhalation or 2 ppm *via* whole body inhalation) for 20 min: independent experiments using these 2 different approaches produced the same results. Data in this article represent findings from the 5 ppm nose only inhalation with equivalent findings observed in the replication cohort exposed to 2 ppm whole body inhalation. Vehicle or 1400 W was administered 1 h before and 6 h after phosgene exposure. For systemic administration, 20 mg/kg of 1400 W was injected subcutaneously. This dose and timing was based upon our and other investigators' prior experience with systemic NOS-2 inhibition (Grant et al., 2009; Hu et al., 2004; Thomsen et al., 1997). For direct lung administration, 1400 W was generated from a 10 mg/ml solution in saline. The exposure atmosphere was generated at 20 psi from a Pari LC Plus nebulizer into a nose only flow past exposure chamber. The chamber flow was 5.0 l/min, and the chamber pressure was ambient as controlled by demand dilution. Filter samples were collected on Pallflex Fiberfilm film filters at a flow rate of 1.0 l/min. The aerosol concentration for the entire exposure was determined to be 0.405 mg/l with a particle size of 0.87 μm MMAD. Oxygen was monitored for each exposure to ensure levels did not drop below 18%. Mice were placed in nose only tubes for 1400 W exposure. Exposures were conducted for 30 min. The dose of aerosolized 1400 W was extrapolated from the SQ dose and was consistent with standard therapeutic delivery calculations for aerosolized pharmaceuticals (Alexander et al., 2008). The animals were euthanized and necropsied 24-h postphosgene exposure. At necropsy, the left lung was fixed by inflation with 10% neutral buffered formalin solution (Sigma-Aldrich) for histopathological analysis. Bronchoalveolar lavage (BAL) fluid collection followed by lung tissue collection for RNA extraction was performed on the right lung. The BAL fluid was centrifuged at 500 g for 5 min and analyzed for total protein concentration using Pierce BCA Protein Assay Kit (Thermo Scientific). Cells recovered from BAL fluid were counted using a hemacytometer and used for cytospin preparations (25 000 or less viable cells/slide). These cytospin slides were stained with the Baxter

Diff-Quick kit (VWR Scientific Products, San Francisco, CA), and the differentials were calculated.

In vitro studies. The A549 human alveoli-derived adenocarcinoma cell line (ATCC) was cultured in F12-K medium (ATCC) supplemented with 10% fetal bovine serum (Gibco) and 1000 U/ml Pen-strep (Lonza). HBEC-2 and HBEC-3 human bronchial epithelial cells (Ramirez *et al*., 2004, a gift From Dr Steven Belinsky, Lovelace Respiratory Research Institute) were cultured in Keratinocyte-SFM combo medium (Gibco). The cells were grown at 37°C in a humidified 5% CO_2 atmosphere in T-75 flasks and subcultured for up to 20 passages. For experimental purposes, the cells were seeded onto 24- or 12-well plates and cultured until they reached full confluence. Additionally, A549 cells were maintained in full confluence for 3 days to reach a stable nondividing state before beginning experiments. For the experiments involving treatment with an NO donor, the cells were incubated with the culture medium containing either vehicle (0.01 N NaOH) or NO-donor diethylenetriamine (DETA) NONOate (Cayman Chemical) at concentrations of 0.1, 0.5, or 1 mM. The cells were harvested for RNA extraction after 24 h of exposure. For the assessment of toxicity induced by DETA NONOate, the cells (both attached and floating) were collected, washed with PBS, and stained with 10 μg/ml propidium iodide (PI) solution in PBS. Next, the relative number of living cells (low fluorescence-emitting population) and dead cells (high fluorescence-emitting population) was assessed by flow cytometric analysis at the emition wavelength 617 nm. For the NOS-2 overexpression experiments, the cells were transfected with empty, GFP-coding or NOS-2-coding plasmids (pReceiver-M02-based DNA plasmids; GeneCopoeia) using Lipofectamine 2000 (Life Technologies) according to the manufacturer's standard protocol. The cells were harvested for RNA isolation 24 h after transfection.

Immunohistochemical and immunofluorescent staining of lung tissue samples. Fresh lung tissue fixed with 10% neutral buffered formalin solution was sequentially incubated with 30 and 70% histologic grade ethanol and underwent routine processing for paraffin embedding. From the paraffin-embedded samples, 5 μm sections were cut, immersed in several changes of xylene, rehydrated in graded alcohols, and washed in PBS. Antigen retrieval was then performed by heating the slides in citrate buffer (pH 6.0) for 10 min. After cooling, the slides were blocked in 5% natural goat serum, 3% bovine serum albumin, and 0.1% Tween-20 in PBS. The slides were incubated with the primary antibody at 4°C overnight. Primary anti-SP-B (Seven Hills Bioreagents), anti-NOS-2 (Millipore), anti-ZO-1 (Abcam), and anti-nitrotyrosine (Millipore) antibodies were used for detection of surfactant protein B (SP-B), NOS-2, zonula occludens 1 (ZO-1), and the total level of nitrotyrosine, respectively. For immunohistochemical staining, after incubation with primary antibodies the slides were washed with PBS; incubated with a goat anti-rabbit biotinylated secondary antibody (Vector Laboratories) for 2 h at room temperature (RT); and then washed with PBS and incubated with avidin-biotin complex (Vector Laboratories) for 30 min at RT. The slides were developed using 0.025% diaminobenzidene (Vector Laboratories) in PBS with 0.1% H_2O_2, counterstained using methyl green (see Figs. 1 and 4) or hematoxylin and eosin (see Fig. 5), and coverslipped using Vectashield mounting medium (Vector Laboratories). For immunofluorescent staining, after incubation with primary antibodies the slides were washed with PBS; incubated with goat anti-rabbit Alexa Fluor 635-conjugated secondary antibody (Invitrogen) for 2 h at RT; and washed with PBS, treated with 4′,6-diamidino-2-phenylindole (DAPI) for nuclear counterstaining, and coverslipped using Vectashield mounting medium (Vector Laboratories). Quantitative analysis of nitrotyrosine staining intensity was performed using Slidebook 5.0 and ImageJ.

Quantitative real-time RT-PCR analysis. Total RNA was isolated from frozen lung tissue samples or cultured cells using an RNeasy Mini Kit (Qiagen) according to the manufacturer's standard protocol. During the isolation process, samples were incubated with DNase I (Qiagen) for 15 min at RT. The concentration and purity of the isolated RNA was assessed using a NanoDrop 2000 spectrophotometer (Thermo Scientific). TaqMan RT-PCR using QuantiTect Virus Kit (Qiagen) was performed in an ABI Prism 7300 Sequence Real-Time PCR System (Applied Biosystems) using universal thermal cycling parameters. Commercially available mouse-specific or human-specific TaqMan gene expression assays (Applied Biosystems) were used to measure the mRNA levels for SP-B, ZO-1, NOS-2, and 18S rRNA. Each sample was run in duplicate. Gene expression was analyzed using the comparative CT method with 18S rRNA as the endogenous control.

Statistical analysis. The results for each treatment group are summarized as the mean value ± SEM. Comparisons of results between different groups were performed using Student's *t*-test, or 1-way ANOVA test followed by Dunnett's post-test (GraphPad Prism 5.04). Statistical significance was defined as a P-value < 0.05 (*), < 0.01 (**), or < 0.001 (***).

RESULTS

NOS-2 Expression Is Increased in the Lung After Phosgene-Induced ALI

We first characterized the extent of lung injury and NOS-2 lung expression induced by phosgene in our experimental mouse model. The phosgene-exposed animals had marked disruption of alveolar epithelial integrity with significant increases in BAL protein (approximately 17-fold) compared with the filtered air controls (170 vs 10 mg/dl, respectively) (Fig. 1A). In addition, histological analysis of lung tissues from the phosgene-exposed animals demonstrated evidence of alveolar edema and inflammatory cell infiltration consistent with lung injury (Figs 1D and 2F). Furthermore, marked increases in NOS-2 expression were observed in the lung following phosgene exposure (Fig. 1B–D). Although NOS-2 was minimally expressed in the lungs of the filtered air-exposed control animals, the phosgene-exposed animals had more than a 20-fold induction of NOS-2 expression in the lung (Fig. 1B). Similarly, immunohistochemical staining of the lung demonstrated minimal NOS-2 expression in control animals, but significant increases in NOS-2 staining in both epithelial and inflammatory cells in the phosgene-exposed animals were observed (Fig. 1C and D). These results demonstrate that NOS-2 is significantly induced in the lung following phosgene exposure. We therefore set out to determine whether NOS-2 plays a role in phosgene-induced ALI.

Aerosolized 1400 W Mitigates Phosgene-Induced Lung Injury

We next investigated whether selective inhibition of NOS-2 with 1400 W would abrogate phosgene-induced lung injury. Two modes of 1400 W administration were used: systemic delivery *via* subcutaneous (SQ) injection and lung-targeted delivery

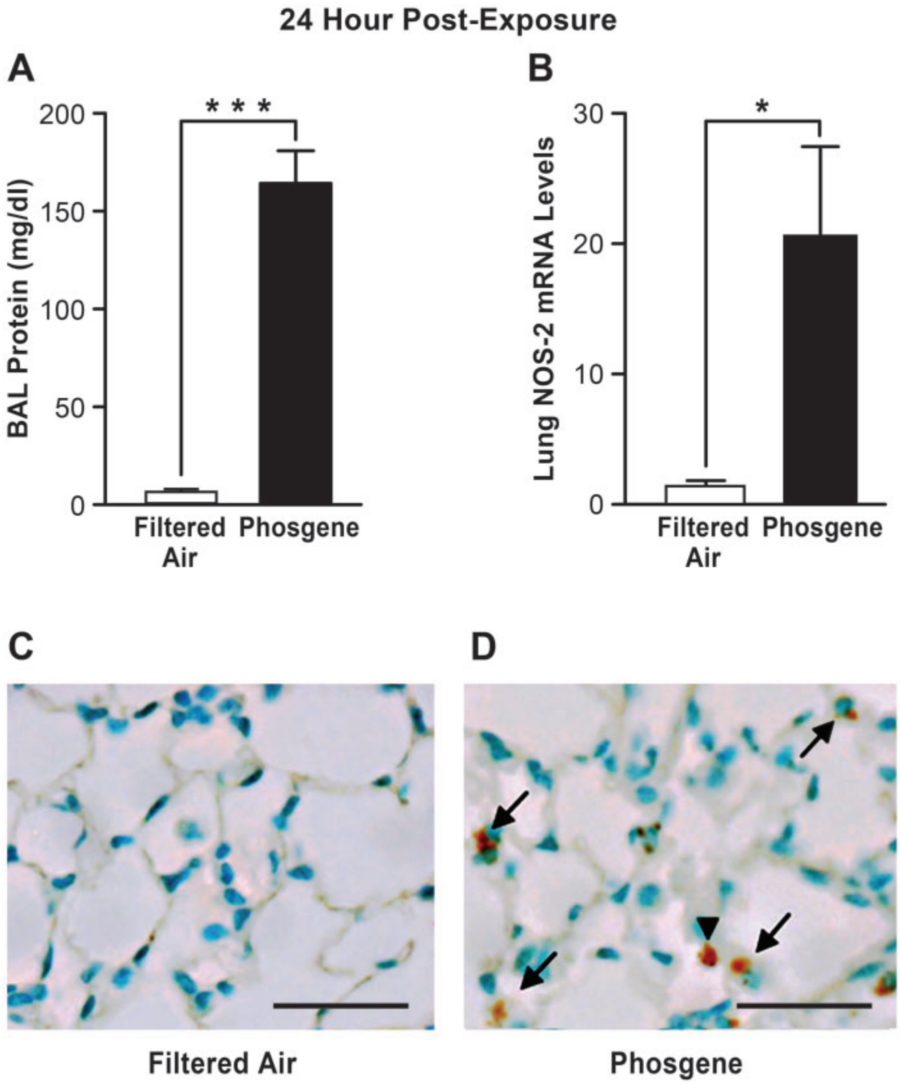

FIG. 1. Lung NOS-2 expression is elevated during phosgene-induced ALI. Mice were exposed to filtered air or phosgene and assessed for lung injury by measuring BAL fluid protein levels **(A)** and NOS-2 expression (relative to the 18S control) was measured by real time qPCR 24 h after phosgene exposure **(B)** ($n = 5$; mean ± SEM, P-value $^{*} < 0.05$, $^{***} < 0.001$). Lungs of mice exposed to filtered air **(C)** or phosgene **(D)** were stained for NOS-2 protein 24 h after exposure (positive epithelial staining is indicated by arrows and positive inflammatory cell staining is indicated by arrowheads, scale bar corresponds to 50 μm).

via inhalation of aerosolized 1400 W. In both models, 1400 W was administrated 1 h before and 6 h after phosgene exposure. At 24 h after phosgene inhalation, the vehicle-treated animals developed significant alveolar leak with a robust increase in BAL protein, which was significantly attenuated in the animals treated with aerosolized 1400 W (Fig. 2B). In contrast, systemically administered 1400 W had no beneficial effect on epithelial barrier integrity (Fig. 2A), supporting the concept of mediation of protection *via* inhibition of NOS-2 expression in the lung epithelium. The increase in the BAL protein content after phosgene exposure was accompanied by a mild but statistically important increase in BAL total cell count (predominantly macrophages; >99% of all BAL fluid cells) after phosgene exposure. Although no significant differences in cell count between the vehicle- and 1400 W-treated animals exposed to phosgene were found, there was a trend toward a decrease in overall cell count in animals exposed to aerosolized 1400 W that was not observed in the animals exposed to systemic 1400 W (Figs. 2C and D). Histologic analysis of the lung tissue revealed marked alveolar wall damage, hemorrhage, and leukocyte infiltration in the vehicle-treated animals following phosgene exposure (Fig. 2F), and a significant attenuation of these responses in the animals treated with aerosolized (Fig. 2G), but not systemic (data not shown) 1400 W. Taken together, these data indicate that lung-targeted delivery of 1400 W *via* inhalation, but not by systemic administration, mitigates phosgene-induced alveolar barrier disruption and development of ALI.

Inhaled 1400 W Inhibits Nitrotyrosine Accumulation in the Lung Following Phosgene Exposure

To confirm that the beneficial effects of aerosolized 1400 W are directly related to NOS-2 enzymatic inhibition, we analyzed lung nitrotyrosine levels. Nitrotyrosine is formed in cells as the final product of NO reactions, and enhanced NOS-2 activity has been reported as the main factor leading to nitrotyrosine synthesis within the injured and inflamed lung (Cho and Chae, 2003; Giaid *et al.*, 2003). Immunofluorescent staining of lungs from filtered air-exposed control animals revealed low levels of nitrotyrosine in both the airways and lung parenchyma (Fig. 3C and D). Following exposure to phosgene, the nitrotyrosine levels

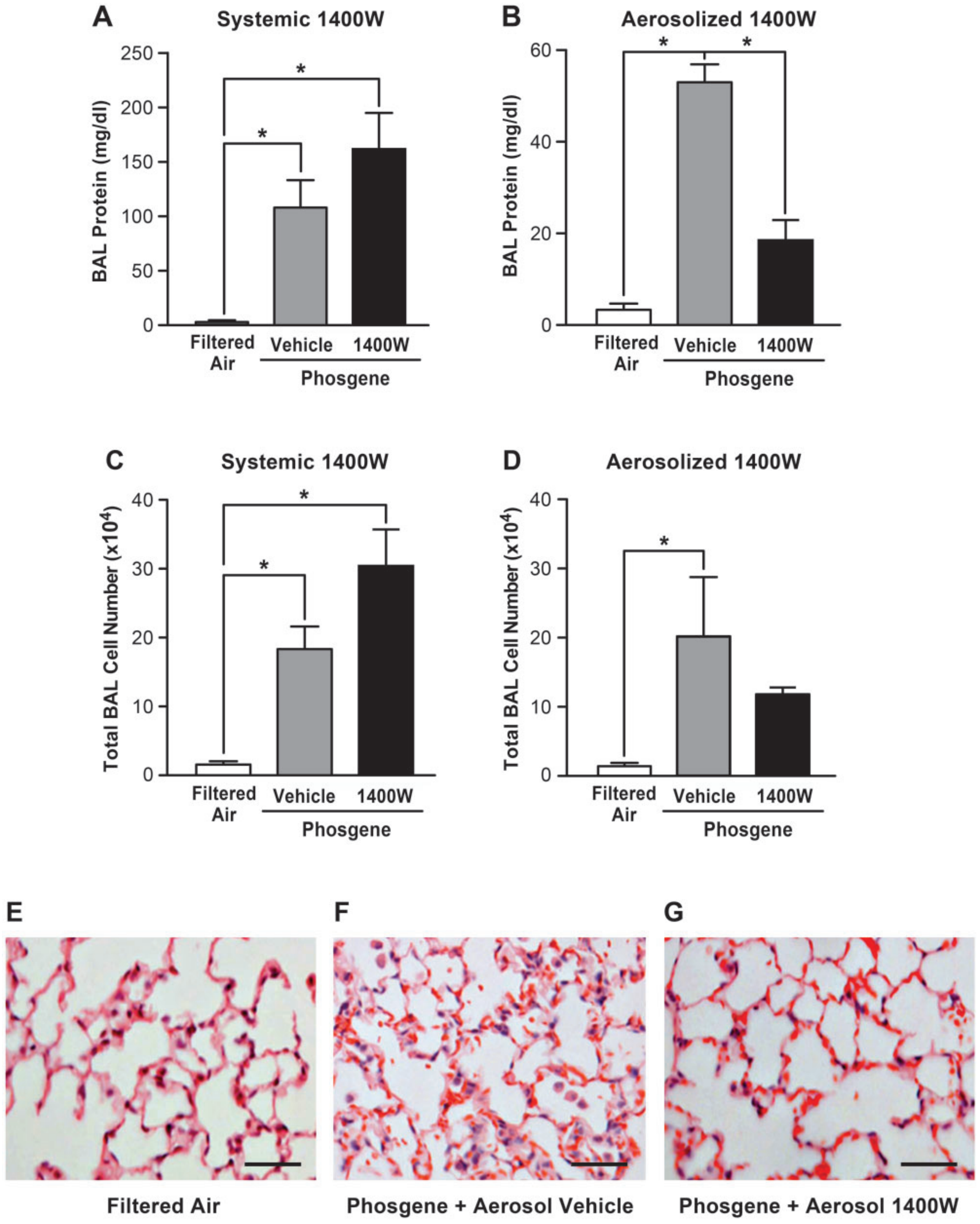

FIG. 2. Inhaled 1400 W mitigates phosgene-induced lung injury, while there is no beneficial effect after systemic 1400 W delivery. Mice were exposed to filtered air or phosgene, with administration of systemic 1400 W or vehicle (PBS) **(A, C)** or inhaled 1400 W or vehicle (PBS) **(B, D)**, and harvested 24 h after exposure. The level of protein in BAL fluid (upper panel) and total BAL cell number (middle panel) were analyzed ($n = 5$; mean ± SEM, P-value $^* < 0.05$). Mice exposed to filtered air **(E)** versus phosgene-aerosolized vehicle **(F)** versus phosgene + aerosolized 1400 W **(G)** were analyzed for histological signs of lung injury (scale bar corresponds to 50 μm).

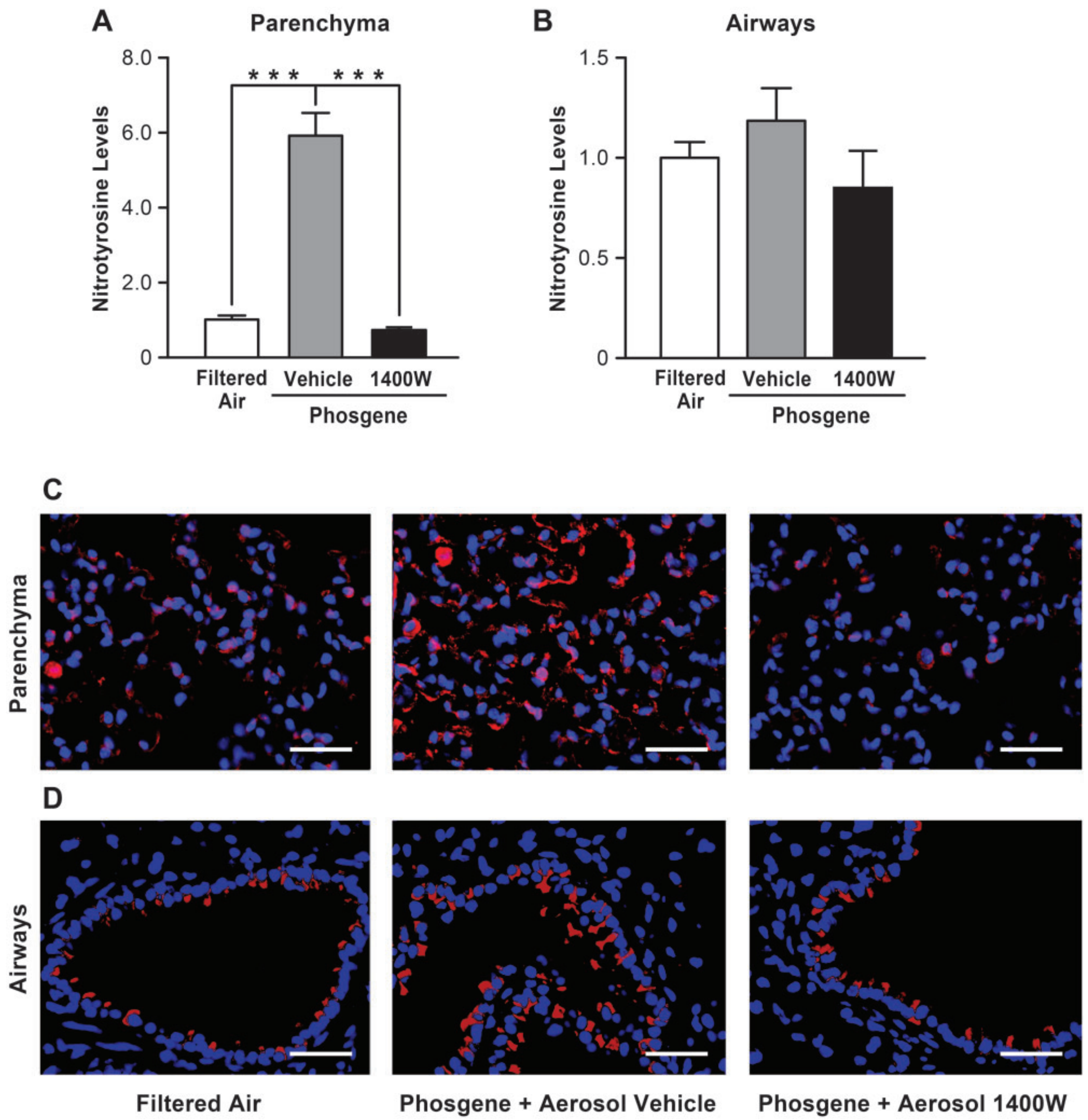

FIG. 3. Inhaled 1400 W inhibits nitrotyrosine accumulation within the lung injured with phosgene. Mice exposed to filtered air, phosgene + inhaled vehicle (PBS) or phosgene + inhaled 1400 W were euthanized 24 h after exposure, and the lungs were stained for nitrotyrosine. Images of the alveolar parenchyma **(C)** and the airways **(D)** were captured (scale bar corresponds to 50 μm), and the intensity of nitrotyrosine staining for alveolar parenchyma **(A)** and airways **(B)** was assessed using ImageJ ($n = 30$ pictures captured of the lungs from 3 mice per experimental condition were analyzed, mean ± SEM, P-value *** < 0.001).

within the lung were increased compared with control animals. Positive staining was detected not only within infiltrating leukocytes, but also within alveolar epithelial cells. Treatment of phosgene-exposed mice with aerosolized 1400 W protected the animals against the nitrotyrosine accumulation within the lung, reducing it to the level observed in control animals. Quantitative analysis of the staining intensities confirmed significantly higher nitrotyrosine staining in the lung parenchyma of the phosgene-exposed mice compared with filtered air controls and phosgene-exposed animals treated with inhaled 1400 W (Fig. 3A). A similar trend was observed for nitrotyrosine accumulation within the airways (Fig. 3B); however, these changes were not statistically significant. Taken together, these results indicate that inhalational delivery of the NOS-2 specific inhibitor 1400 W reaches the distal lung parenchyma and efficiently blocks nitrotyrosine synthesis triggered by phosgene exposure.

The NOS-2 Inhibitor 1400W Augments Expression of SP-B

We previously demonstrated in a murine inhaled endotoxin-induced ALI model that NOS-2-derived NO downregulates transcription of SP-B, which is critical for maintaining alveolar

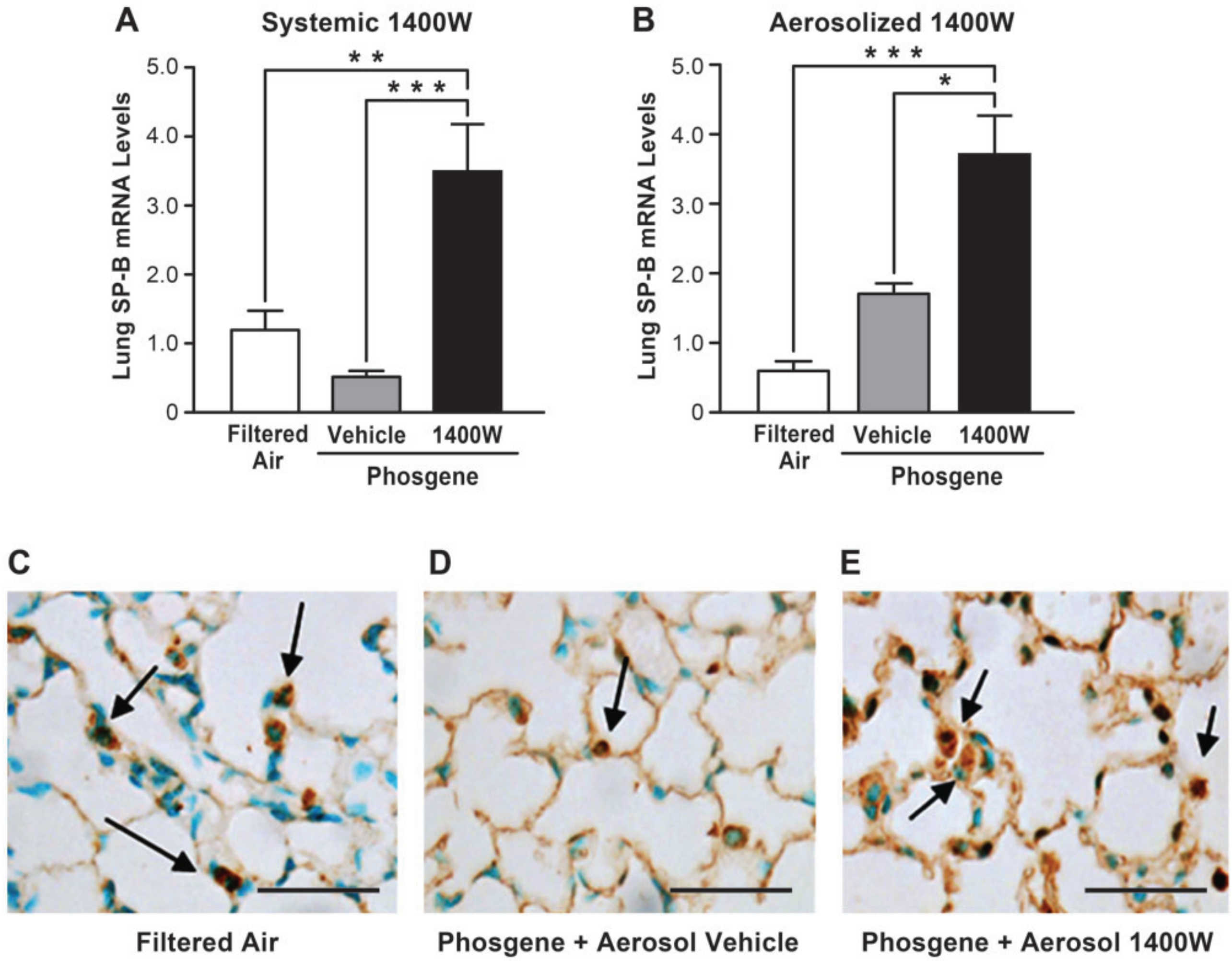

FIG. 4. The NOS-2 inhibitor 1400 W augments levels of the critical protein SP-B. Mice were exposed to phosgene or filtered air, administered with 1400 W or vehicle (PBS) systemically **(A)** or by inhalation **(B)**, and euthanized 24 h later. The mice were analyzed for SP-B mRNA levels by real time qPCR ($n = 5$, mean ± SEM, P-value $^{*} < 0.05$, $^{**} < 0.01$, $^{***} < 0.001$). Lungs harvested from mice subjected to filtered air **(C)**, phosgene + aerosolized vehicle **(D)** or phosgene + aerosolized 1400 W **(E)** were stained for SP-B (examples of positive staining in lung epithelial cells indicated by arrows, scale bar corresponds to 50 μm).

surface tension and surfactant function (Baron *et al.*, 2004a). Thus, we investigated the effects of phosgene-induced NOS-2 on SP-B expression. Real-time qPCR analysis demonstrated a trend towards decrease in SP-B mRNA levels in the lung exposed to phosgene compared with filtered air controls; however, this change was not statistically significant (Fig. 4A). In contrast, systemic administration of 1400 W elevated the levels of the SP-B transcript approximately 3-fold in comparison with the filtered air-exposed animals. Treatment of the phosgene-exposed animals with aerosolized 1400 W elevated the SP-B transcript to a greater degree (~8-fold higher than in the animals exposed to filtered air, Fig. 4B). Although a trend towards elevated SP-B expression in phosgene-exposed animals that inhaled the aerosolized vehicle could also be seen, this change was not statistically significant. Immunohistochemical staining demonstrated a decrease in the SP-B protein level in the lung parenchyma after phosgene exposure that was rescued following treatment with aerosolized 1400 W (Fig. 4C–E). These data indicate that 1400 W augments SP-B gene expression following phosgene exposure and thus may account for part of the mechanism of protection of 1400 W from phosgene-induced ALI. Although the increase in SP-B mRNA level was more profound with aerosolized 1400 W, this effect was not only due to the direct delivery of 1400 W to the lung epithelium, but may also relate to potential beneficial effects of delivery of aerosolized PBS in the setting of phosgene-induced ALI as indicated by the nonsignificant increase in SP-B expression with aerosolized PBS alone.

Inhaled 1400 W Restores Expression of ZO-1 in Lungs of phosgene-exposed animals

Because phosgene exposure led to a dramatic loss of alveolar epithelial integrity and inhalation of 1400 W attenuated epithelial barrier disruption, we next investigated whether expression of tight junction proteins known to be important for barrier function in the lung was altered in the phosgene-exposed animals. Real-time qPCR analysis revealed that phosgene exposure significantly decreased expression of the tight junction protein ZO-1. Administration of aerosolized 1400 W to the phosgene-exposed animals significantly attenuated the loss of ZO-1 expression in the lung following phosgene exposure (Fig. 5B). Similar to the effects of 1400 W on the BAL protein leak, systemic administration of 1400 W was not protective against downregulation of ZO-1 in the lung in response to phosgene

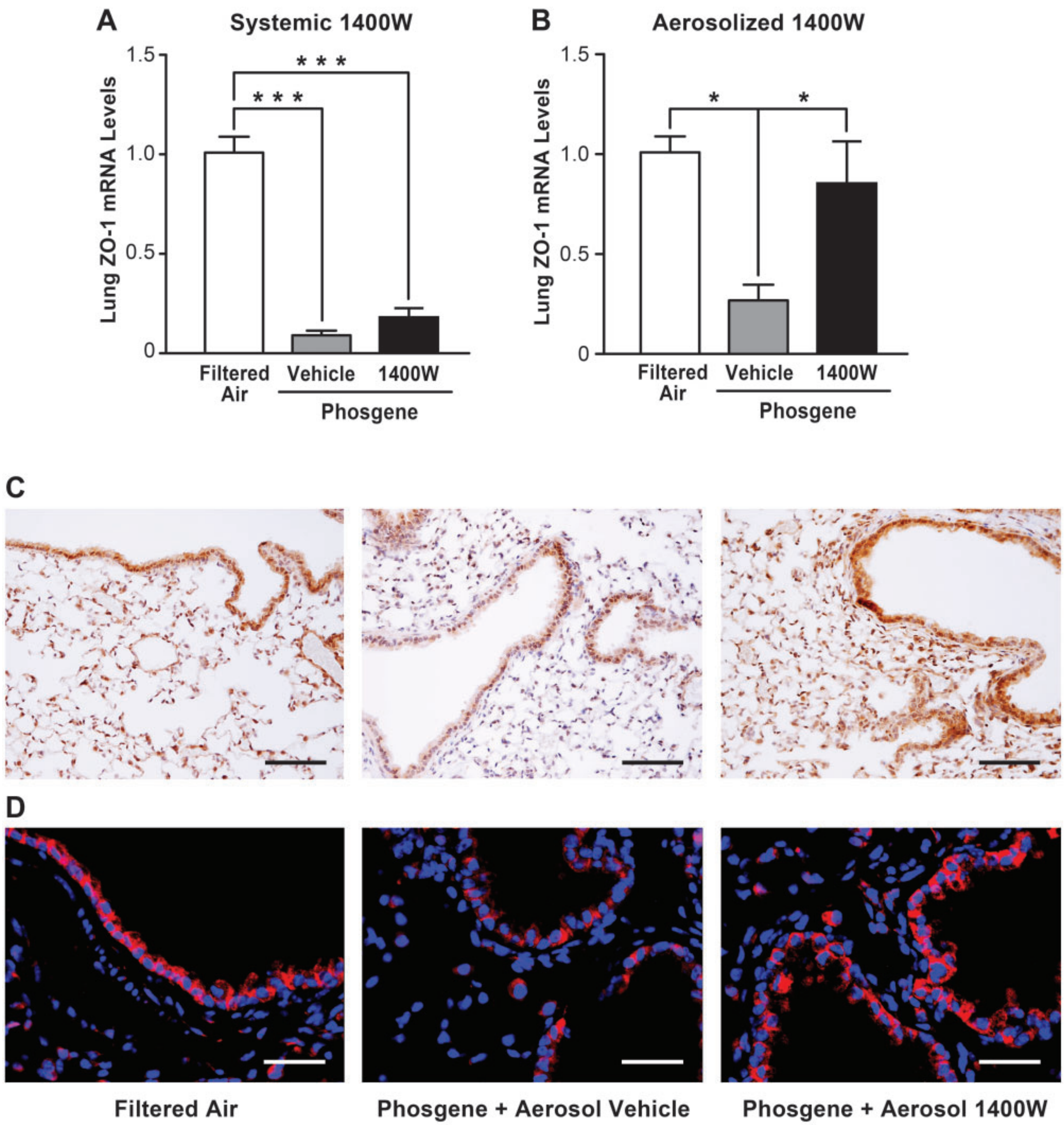

FIG. 5. Inhalation of 1400 W restores expression of the tight junction protein ZO-1 after phosgene-induced lung injury. Mice were exposed to phosgene or filtered air, administered with 1400 W or vehicle (PBS) systemically **(A)** or by inhalation **(B)**, and euthanized 24 h later. The lung tissues were analyzed for ZO-1 mRNA levels by real time qPCR ($n = 4$, mean ± SEM, P-value $^* < 0.05$, $^{***} < 0.001$). Lung sections from animals exposed to filtered air, phosgene + aerosolized vehicle or phosgene + aerosolized 1400 W were stained for ZO-1 protein by immunohistochemistry and counterstained with hematoxylin (**C,** scale bar corresponds to 150 μm), or stained by immunofluorescence (red) and counterstained with DAPI (blue) (**D,** scale bar corresponds to 50 μm).

inhalation (Fig. 5A). Furthermore, immunohistochemical staining demonstrated reduced protein expression of ZO-1 in phosgene-treated animals and the restoration of the ZO-1 expression in animals treated with inhaled 1400 W (Fig. 5C). Immunofluorescent staining for ZO-1 confirmed these findings and did not demonstrate any clear differences in the localization of ZO-1 expression in the lungs of the animals following phosgene exposure or inhaled 1400 W treatment, further confirming that a reduced expression rather than relocalization of ZO-1 was correlated with the observed injury (Fig. 5D). Taken together, our data suggest that phosgene exposure disrupts alveolar epithelial integrity, at least in part, by NOS-2-dependent downregulation of ZO-1 gene expression.

NOS-2-Derived NO Downregulates ZO-1 Gene Expression in Human Lung Epithelial Cells

A previous study reported that NO and its products can disrupt tight junctions between cells within the lung and the intestinal epithelium (Salzman *et al.*, 1995). Our results now suggest that reactive nitrogen species generated by NOS-2 play an important role in disrupting tight junction homeostasis in phosgene-induced ALI *via* downregulation of ZO-1 expression at the transcriptional level. To directly test the role of NO in the disruption of tight junctions due to regulation of ZO-1 transcription, we performed *in vitro* experiments using the human alveolar-like cell line A549 and 2 noncancerous cell lines derived from human bronchial epithelium, HBEC-2 and HBEC-3. These cells were exposed to reactive nitrogen species by incubation with the NO donor DETA NONOate for 24 h. Treatment with DETA NONOate led to a dose-dependent decrease in ZO-1 mRNA levels in all 3 epithelial cell lines (Fig. 6A). Importantly, the concentrations of DETA NONOate used (0.1, 0.5, and 1 mM) did not result in substantial loss of cell viability as measured by PI exclusion testing (Supplementary Fig. S1A). Therefore, the NO-associated downregulation in ZO-1 expression in lung epithelial cells is not secondary to a nonspecific shutdown of transcription associated with cell death.

We further confirmed the effect of NOS-2-derived NO on ZO-1 expression in lung epithelial cells that overexpressed NOS-2. Human A549, HBEC-2, and HBEC-3 cells were transfected with an empty plasmid or a plasmid carrying an open reading frame for NOS-2 under the control of a constitutively expressed promoter. Transfection efficacy, assessed by microscopic visualization of cells transfected with a GFP-coding plasmid of comparable length and structure, demonstrated 5-10% positively transfected cells (Fig. 6B). This was accompanied by an approximately 200- to 700-fold increase in NOS-2 transcript level over the empty plasmid-transfected control (Supplementary Fig. S1B). Despite the low number of positively transfected cells, overexpression of NOS-2 led to a significant decrease in ZO-1 mRNA levels in all 3 lung epithelial cells compared with empty plasmid-transfected control cells (Fig. 6C), which indicates that NOS-2-derived NO downregulates expression of the tight junction gene ZO-1 at the transcriptional level in these lung epithelial cells. Taken together, our *in vivo* and *in vitro* findings demonstrate that phosgene-induced NOS-2 plays a key role in the pathogenesis of phosgene-induced ALI and suggest that inhalation of a selective NOS-2 inhibitor abrogates the NOS-2-derived NO-induced epithelial barrier disruption.

DISCUSSION

This study was designed to investigate the role of NOS-2 in the development of acute and severe injury of the lung as a consequence of phosgene exposure. In order to investigate whether inhibition of NOS-2 has beneficial effects in mice exposed to this toxic gas, we used 1400 W, a small molecule inhibitor highly specific for NOS-2, which does not affect the function of the 2 other constitutively expressed isoforms, nNOS and eNOS (Garvey et al., 1997). By testing 2 different routes of delivery of 1400 W (systemic administration and direct delivery to the lungs), our goal was to optimize administration of 1400 W for effective pharmaceutical intervention against phosgene-induced ARDS. This approach was based on our previous data demonstrating that localized expression of NOS-2 in the lung epithelium plays an important role in lung injury mediated by inhaled endotoxin (Baron et al., 2004a).

NOS-2 Inhibition Alleviates Phosgene-Induced Lung Injury

NO produced by NOSs is one of the critical mediators of ARDS caused by a variety of biological, mechanical, and chemical factors, including toxic gas exposure. Of the 3 NOS isoforms transcribed in mammals, the inducible isoform (NOS-2), rather than the constitutively expressed eNOS and nNOS, has been described as the main driver of NO-mediated lung injury. We have previously demonstrated a critical role for lung parenchyma-derived NOS-2 in the development of endotoxin-induced lung injury. The absence of NOS-2 in lung parenchyma cells, but not the absence from bone marrow-derived leukocytes, protects mice from the physiological lung dysfunction and SP-B gene dysregulation induced by endotoxin (Baron *et al.*, 2004a).

Recent studies have shown that NOS-2 is upregulated in the lungs of rats exposed to phosgene (Chen *et al.*, 2013; Zhang *et al.*, 2012). Additionally, elevated exhaled NO levels have been reported in rats following phosgene inhalation (Li *et al.*, 2013). Our study now also reveals that NOS-2 expression is significantly upregulated in the lung at the mRNA and protein levels in mice 24 h after phosgene exposure.

Our data also indicate that epithelial cells are likely a key source of NOS-2 expression within the lung after phosgene exposure. Immunostaining of lung sections from phosgene-exposed animals demonstrated upregulation of NOS-2 expression in alveolar leukocytes and epithelial cells, with more predominant staining observed in lung epithelial cells. Although the infiltrating leukocytes observed in the lung parenchyma of the phosgene-exposed mice stained positive for NOS-2 (Fig. 1D), low overall levels of inflammation were observed in BAL fluid 24 h after phosgene exposure, and histologically there was only a mild increase in inflammation at this time. Moreover, immunostaining for nitrotyrosine, a major product of protein nitration by peroxynitrite, demonstrated that nitrotyrosine accumulation was present within the macrophage-free regions of the lung parenchyma, further supporting the concept that epithelial cells are an important source of NOS-2-derived NO in the lung following phosgene exposure. Given the direct injury to the lung epithelium caused by phosgene and the localized NOS-2 expression in this compartment, targeted inhalational therapies directed at the alveolar epithelium represent an important therapeutic avenue.

Based on these findings, we investigated whether administration of a selective NOS-2 inhibitor would attenuate phosgene-induced lung injury and, in particular, whether aerosolized administration would prove superior to systemic delivery. In contrast to inducible NOS-2, disruption of nNOS and eNOS enzymatic activity may be deleterious to several organs by disrupting the homeostasis of the vascular endothelium and central nervous system (Balakumar *et al.*, 2012; Wang and Golledge, 2013). Therefore, the lack of specificity of many NOS inhibitors, including L-NAME and L-NIL, may outweigh potential beneficial effects of these agents on NOS-2 inhibition due to inhibition of eNOS and nNOS activity. Previous studies have evaluated the effects of non-specific NOS inhibition on phosgene-induced abnormalities in cardiopulmonary reflexes in rats (Zhang *et al.*, 2012). Administration of L-NAME, a nonspecific inhibitor of all NOS isoforms, and L-NIL, a NOS-2 inhibitor with poor specificity, had no beneficial effects on pulmonary edema, cardiac function, or body and lung weights. Moreover, treatment with L-NAME was shown to aggravate some of the deleterious effects caused by phosgene (Zhang *et al.*, 2012).

In this study, we chose the highly specific inhibitor of NOS-2, 1400 W. It exhibits K_i values of 7 nM, 2 μM, and 50 μM for human NOS-2, nNOS, and eNOS enzymes, respectively with at least 1000-fold selectivity for iNOS versus eNOS in rat tissue (Garvey *et al.*, 1997), whereas the previously studied NOS inhibitor L-NIL (Zhang *et al.*, 2012) exhibits IC_{50} values of 3.3 μM for NOS-2

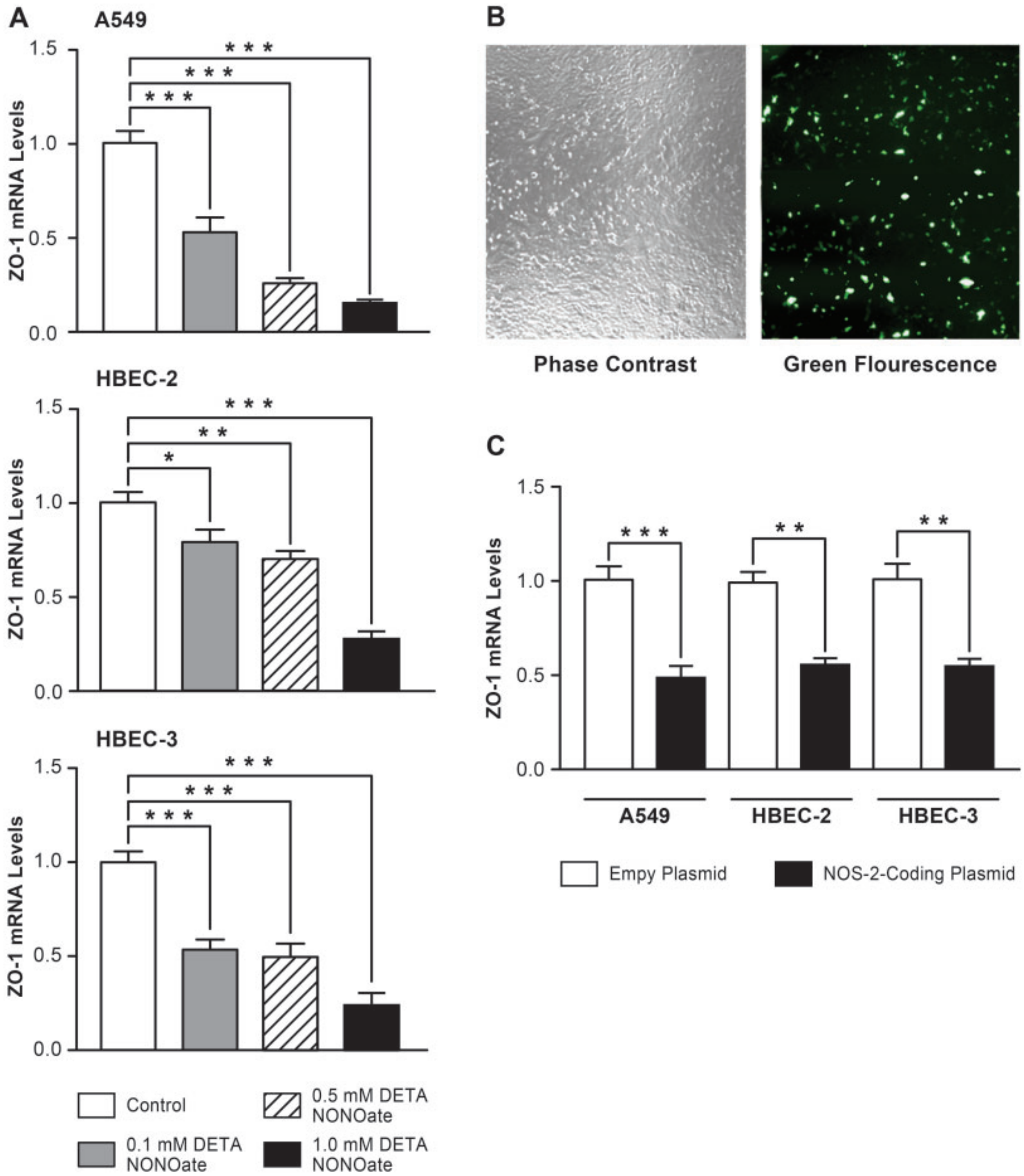

FIG. 6. NOS-2-derived NO downregulates ZO-1 gene expression in human lung epithelial cells *in vitro*. A549, HBEC-2 and HBEC-3 lung epithelial cells were incubated with the NO donor DETA NONOate (0.1, 0.5, or 1 mM) for 24 h, harvested for RNA isolation and analyzed for ZO-1 mRNA levels using real time qPCR **(A)** ($n = 4$, mean ± SEM). A549, HBEC-2, and HBEC-3 cells were transfected with empty, GFP-coding or NOS-2-coding plasmids. Transfection efficacy was estimated by microscopic observation of the GFP-coding plasmid transfected cells **(B)**. Cells transfected with empty or NOS-2-coding plasmids were harvested for RNA isolation and analyzed for the ZO-1 mRNA levels using real time qPCR **(C)** ($n = 4$, mean ± SEM). For both **(A)** and **(C)** statistical significane is defined as a *P*-value * < 0.05, ** < 0.01, or *** < 0.001.

(mouse) and 92 μM for nNOS (rat) making it much less specific and less effective than 1400 W. We investigated whether treatment with 1400 W would attenuate phosgene-induced lung injury and, furthermore, whether lung-targeted delivery of 1400 W would be more efficacious than systemic delivery. Our findings reveal that inhalation, but not systemic delivery, of 1400 W leads to dramatic reductions in vascular leak and lung injury caused by phosgene. These results indicate that the specificity of 1400 W for NOS-2 and the route of administration both play key roles in attenuating the phosgene-induced epithelial barrier disruption and development of lung injury. Our results support the premise that systemic inhibition of NOS-2 may not be universally beneficial, and in fact it may be harmful in some settings due to the pleiotropic effects of NOS-2 in different tissues and cell types and under different disease conditions (Kubes, 2000). Because to date there have been no reports of successful targeted therapy for phosgene-induced lung injury, this approach of targeted NOS-2 inhibition by aerosolized delivery of a specific NOS-2 inhibitor raises an important avenue of novel therapy to ameliorate the exceedingly high mortality observed for this condition.

Phosgene-Induced NOS-2 Regulates SP-B and ZO-1 Expression

To elucidate the mechanism underlying the beneficial effects of NOS-2 inhibition in phosgene-induced ALI, we investigated whether 1400 W altered expression of SP-B and the tight junction protein ZO-1, 2 proteins critical for maintenance of normal lung function and epithelial barrier integrity. Several animal studies have previously demonstrated that NO may cause surfactant dysfunction (Baron *et al*., 2004a; Haddad *et al*., 1994;

Hallman and Bry, 1996; Matalon *et al.*, 1996). Furthermore, phosgene has been shown to disrupt alveolar surfactant homeostasis by oxidative damage to the lipid and peptide residues (Haddad *et al.*, 1993). Additionally, we previously reported that NO directly affects SP-B expression *via* NOS-2-dependent downregulation of SP-B at the transcriptional level (Baron *et al.*, 2004a). In this study, we now demonstrate that selective inhibition of NOS-2 with 1400 W augments SP-B expression in the lung following phosgene inhalation. Interestingly, we also found that treatment with aerosolized PBS alone caused a nonsignificant increase in SP-B expression in animals exposed to phosgene. Although the mechanism underlying this effect is not completely understood, we speculate that inhaled PBS treatment may, in part, provide a protective barrier against phosgene due to the poor solubility of this gas in aqueous solutions, or due to rapid hydrolysis of phosgene in water to chlorine and carbon dioxide. Thus, there may be multiple modes of benefit in inhaled therapeutics for phosgene-induced lung injury.

Furthermore, aerosolization of 1400 W rescued expression of the critical tight junction protein ZO-1 and attenuated epithelial barrier disruption in mice exposed to phosgene. Previous work in a mouse endotoxemia model and in cytokine-stimulated bronchiolar epithelial cells showed that tight junction dysregulation may be NO-dependent, but details and specific targets of the mechanistic underpinnings of this observation were not reported (Han *et al.*, 2004a). In addition, several studies have reported that NOS-2-derived NO can disrupt tight junctions leading to destruction of blood-tissue barrier integrity in several organs including the brain, intestine, and liver (Han *et al.*, 2004b; Mazzon and Cuzzocrea, 2003; Salzman *et al.*, 1995; Thiel and Audus, 2001). However, the mechanism underlying these effects is also not completely understood. Our study shows for the first time that treatment with an NO donor or exogenous NOS-2 overexpression significantly reduces ZO-1 expression in lung epithelial cells in a manner similar to that associated with the phosgene-dependent NOS-2 induction *in vivo*. Taken together, our findings suggest that NOS-2-induced disruption of epithelial tight junctions and barrier dysfunction secondary to phosgene involves downregulation of ZO-1 gene expression mediated by NOS-2-derived NO. Thus, this observation opens up a new avenue of mechanistic understanding regarding barrier disruption in the lung, which is a key component underlying the lung injury induced by toxicants, as well as non-toxicant-mediated ALI.

CONCLUSIONS

Our study demonstrates that NOS-2-derived NO plays a critical role in the development of phosgene-induced ALI. Inhibition of NOS-2 activity using the highly specific inhibitor 1400 W when administered directly to the lung *via* inhalation attenuates the epithelial barrier disruption and lung injury induced by phosgene. Specifically, administration of aerosolized 1400 W preserves epithelial integrity and mitigates phosgene-induced ALI by attenuating the reduction in ZO-1 expression and augmenting expression of SP-B. Taken together, our findings suggest that inhalational delivery of a selective NOS-2 inhibitor represents a promising therapeutic strategy for treatment of phosgene-induced ARDS and may have broader applicability for other forms of chemical as well as non-chemical agent-induced lung injury.

SUPPLEMENTARY DATA

Supplementary data are available online at http://toxsci.oxfordjournals.org/.

FUNDING

This work was supported by Lovelace Respiratory Research Institute/Brigham and Women's Hospital institutional money as part of their consortium, and by the National Institutes of Health (HL091957 to R.M.B.).

ACKNOWLEDGMENT

We thank Thomas Gagliano of LRRI for the graphics artwork.

REFERENCES

Alexander, D. J., Collins, C. J., Coombs, D. W., Gilkison, I. S., Hardy, C. J., Healey, G., Karantabias, G., Johnson, N., Karlsson, A., Kilgour, J. D., and McDonald, P. (2008). Association of Inhalation Toxicologists (AIT) working party recommendation for standard delivered dose calculation and expression in non-clinical aerosol inhalation toxicology studies with pharmaceuticals. *Inhal. Toxicol.* **20**, 1179–1189.

Balakumar, P., Kathuria, S., Taneja, G., Kalra, S., and Mahadevan, N. (2012). Is targeting eNOS a key mechanistic insight of cardiovascular defensive potentials of statins? *J. Mol. Cell. Cardiol.* **52,** 83–92.

Baron, R. M., Carvajal, I. M., Fredenburgh, L. E., Liu, X., Porrata, Y., Cullivan, M. L., Haley, K. J., Sonna, L. A., De Sanctis, G. T., Ingenito, E. P., and Perrella, M. A. (2004a). Nitric oxide synthase 2 down-regulates surfactant protein B expression and enhances endotoxin-induced lung injury in mice. *FASEB J.* **18**(11), 1276-1278.

Baron, R. M., Carvajal, I. M., Liu, X., Okabe, R. O., Fredenburgh, L. E., Macias, A. A., Chen, Y. H., Ejima, K., Layne, M. D., and Perrella, M. A. (2004b). Reduction of nitric oxide synthase 2 expression by distamycin A improves survival from endotoxemia. *J. Immunol.* **173**(6), 4147-4153.

Brown, R. F., Jugg, B. J., Harban, F. M., Ashley, Z., Kenward, C. E., Platt, J., Hill, A., Rice, P., and Watkins, P. E. (2002). Pathophysiological responses following phosgene exposure in the anaesthetized pig. *J. Appl. Toxicol.* **22**, 263–269.

Chen, H. L., Bai, H., Xi, M. M., Liu, R., Qin, X. J., Liang, X., Zhang, W., Zhang, X. D., Li, W. L., and Hai, C. X. (2013). Ethyl pyruvate protects rats from phosgene-induced pulmonary edema by inhibiting cyclooxygenase2 and inducible nitric oxide synthase expression. *J. Appl. Toxicol.* **33**, 71–77.

Cho, W. S., and Chae, C. (2003). Evidence of nitric oxide synthase 2 activity in swine naturally infected with Actinobacillus pleuropneumoniae. *Vet. Pathol.* **40**, 276–282.

Cortés, I., Peñuelas, O., and Esteban, A. (2012). Acute respiratory distress syndrome: Evaluation and management. *Minerva Anestesiol.* **78**, 343–357.

Fan, E., Villar, J., and Slutsky, A. S. (2013). Novel approaches to minimize ventilator-induced lung injury. *BMC Med.* **11**, 85.

Garvey, E. P., Oplinger, J. A., Furfine, E. S., Kiff, R. J., Laszlo, F., Whittle, B. J., and Knowles, R. G. (1997). 1400W is a slow, tight binding, and highly selective inhibitor of inducible nitric-oxide synthase in vitro and in vivo. *J. Biol. Chem.* **272**, 4959–4963.

Giaid, A., Lehnert, S. M., Chehayeb, B., Chehayeb, D., Kaplan, I., and Shenouda, G. (2003). Inducible nitric oxide synthase and nitrotyrosine in mice with radiation-induced lung damage. *Am. J. Clin. Oncol.* **26**, e67–e72.

Grainge, C., and Rice, P. (2010). Management of phosgene-induced acute lung injury. Clin. Toxicol. (Phila). **48**, 497–508.

Grant, M. A., Baron, R. M., Macias, A. A., Layne, M. D., Perrella, M. A., Rigby, A. C. (2009). Netropsin improves survival from endotoxaemia by disrupting HMGA1 binding to the NOS2 promoter. *Biochem. J.* **418**, 103–112.

Guérin, C., Reignier, J., Richard, J. C., Beuret, P., Gacouin, A., Boulain, T., Mercier, E., Badet, M., Mercat, A., Baudin, O., *et al.*; PROSEVA Study Group. (2013). Prone positioning in severe acute respiratory distress syndrome. *N. Engl. J. Med.* **368**, 2159–2168.

Guo, Y. L., Kennedy, T. P., Michael, J. R., Sciuto, A. M., Ghio, A. J., Adkinson, N. F., and Gurtner, G. H. (1990). Mechanism of phosgene-induced lung toxicity: Role of arachidonate mediators. *J. Appl. Physiol.* **69**, 1615–1622.

Haddad, I. Y., Crow, J. P., Hu, P., Ye, Y., Beckman, J., and Matalon S. (1994). Concurrent generation of nitric oxide and superoxide damages surfactant protein A. *Am. J. Physiol.* **267**(3 Pt 1), L242–L249.

Haddad, I. Y., Ischiropoulos, H., Holm, B. A., Beckman, J. S., Baker, J. R., and Matalon, S. (1993). Mechanisms of peroxynitrite-induced injury to pulmonary surfactants. *Am. J. Physiol.* **265**, L555–L564.

Hallman, M., and Bry, K. (1996). Nitric oxide and lung surfactant. *Semin. Perinatol.* **20**, 173–185.

Han, X., Fink, M. P., Uchiyama, T., Yang, R., and Delude, R. L. (2004a). Increased iNOS activity is essential for pulmonary epithelial tight junction dysfunction in endotoxemic mice. *Am. J. Physiol. Lung Cell Mol. Physiol.* **286**, L259–L267.

Han, X., Fink, M. P., Yang, R., and Delude, R. L. (2004b). Increased iNOS activity is essential for intestinal epithelial tight junction dysfunction in endotoxemic mice. *Shock* **21**(3), 261–270.

Hu, D. E., Dyke, S. O., Moore, A. M., Thomsen, L. L., Brindle, K. M. (2004). Tumor cell-derived nitric oxide is involved in the immune-rejection of an immunogenic murine lymphoma. *Cancer Res.* **64**, 152–161.

Kubes, P. (2000). Inducible nitric oxide synthase: A little bit of good in all of us. *Gut.* **47**(1), 6–9.

Li, W., Liu, F., Wang, C., Truebel, H., and Pauluhn, J. (2013). Novel insights into phosgene-induced acute lung injury in rats: Role of dysregulated cardiopulmonary reflexes and nitric oxide in lung edema pathogenesis. *Toxicol. Sci.* **131**, 612–628.

Martin, J. G., Campbell, H. R., Iijima, H., Gautrin, D., Malo, J. L., Eidelman, D. H., Hamid, Q., and Maghni, K. (2003). Chlorine-induced injury to the airways in mice. *Am. J. Respir. Crit. Care. Med.* **168**, 568–574.

Matalon, S., DeMarco, V., Haddad, I. Y., Myles, C., Skimming, J. W., Schürch, S., Cheng, S., and Cassin, S. (1996). Inhaled nitric oxide injures the pulmonary surfactant system of lambs in vivo. *Am. J. Physiol.* **270**(2 Pt 1), L273–L280.

Matthay, M. A., and Zemans, R. L. (2011). The acute respiratory distress syndrome: Pathogenesis and treatment. *Annu. Rev. Pathol.* **6**, 147–163.

Mazzon, E., and Cuzzocrea, S. (2003). Role of iNOS in hepatocyte tight junction alteration in mouse model of experimental colitis. *Cell. Mol. Biol.* **49**, 45–57.

Mehta, S. (2005). The effects of nitric oxide in acute lung injury. *Vascul. Pharmacol.* **43**, 390–403.

Papazian, L., Forel, J. M., Gacouin, A., Penot-Ragon, C., Perrin, G., Loundou, A., Jaber, S., Arnal, J. M., Perez, D., Seghboyan, J. M., *et al.*; ACURASYS Study Investigators. (2010). Neuromuscular blockers in early acute respiratory distress syndrome. *N. Engl. J. Med.* **363**, 1107–1116.

Pauluhn, J. (2006). Acute nose-only exposure of rats to phosgene. Part I: Concentration x time dependence of LC50s, nonlethal-threshold concentrations, and analysis of breathing patterns. *Inhal Toxicol.* **18**, 423–435.

Pauluhn, J., Carson, A., Costa, D. L., Gordon, T., Kodavanti, U., Last, J. A., Matthay, M. A., Pinkerton, K. E., and Sciuto, A. M. (2007). Workshop summary: Phosgene- induced pulmonary toxicity revisited: Appraisal of early and late markers of pulmonary injury from animal models with emphasis on human significance. *Inhal. Toxicol.* **19**, 789–810.

Pheng, L. H., Francoeur, C., and Denis, M. (1995). The involvement of nitric oxide in a mouse model of adult respiratory distress syndrome. *Inflammation* **19**, 599–610.

Ramirez, R. D., Sheridan, S., Girard, L., Sato, M., Kim, Y., Pollack, J., Peyton, M., Zou, Y., Kurie, J. M., Dimaio, J. M., *et al.* (2004). Immortalization of human bronchial epithelial cells in the absence of viral oncoproteins. *Cancer Res.* **64**, 9027–9034.

Saguil, A., and Fargo, M. (2012). Acute respiratory distress syndrome: Diagnosis and management. *Am. Fam. Physician* **85**, 352–358.

Salzman, A. L., Menconi, M. J., Unno, N., Ezzell, R. M., Casey, D. M., Gonzalez, P. K., and Fink, M. P. (1995). Nitric oxide dilates tight junctions and depletes ATP in cultured Caco-2BBe intestinal epithelial monolayers. *Am. J. Physiol.* **268**(2 Pt 1), G361–G373.

Shafeeq, H., and Lat, I. (2012). Pharmacotherapy for acute respiratory distress syndrome. *Pharmacotherapy* **32**, 943–957.

Thiel, V. E., and Audus, K. L. (2001). Nitric oxide and blood-brain barrier integrity. *Antioxid. Redox Signal.* **3**, 273–278.

Thomsen, L. L., Scott, J. M., Topley, P., Knowles, R. G., Keerie, A. J., Frend, A. J. (1997). Selective inhibition of inducible nitric oxide synthase inhibits tumor growth in vivo: Studies with 1400W, a novel inhibitor. *Cancer Res.* **57**, 3300–3304.

Wang, Y., and Golledge, J. (2013). Neuronal nitric oxide synthase and sympathetic nerve activity in neurovascular and metabolic systems. *Curr. Neurovasc. Res.* **10**, 81–89.

Zhang, L., Liu, Q., Yuan, X., Wang, T., Luo, S., Lei, H., and Xia, Y. (2013). Requirement of heat shock protein 70 for inducible nitric oxide synthase induction. *Cell Signal.* **25**, 1310–1317.

Zhang, L., Shen, J., Gan, Z. Y., He, D. K., and Zhong, Z. Y. (2012). Protective effect of melatonin in rats with phosgene-induced lung injury. Zhonghua Lao Dong Wei Sheng Zhi Ye Bing Za Zhi. **30**, 834–838. [Article in Chinese].